Journal of Solid State Chemistry 183 (2010) 527–531

Contents lists available at ScienceDirect

Journal of Solid State Chemistry

journal homepage: www.elsevier.com/locate/jssc

$Ca_{3-x}La_xCo_4O_{9+\delta}$ (x=0, 0.3): New cobaltite materials as cathodes for proton conducting solid oxide fuel cell

Hamdi Ben Yahia, Fabrice Mauvy *, Jean Claude Grenier

CNRS, Université de Bordeaux, ICMCB, 87, Avenue A. Schweitzer, 33608 Pessac Cedex, France

ARTICLE INFO

Article history:
Received 9 September 2009
Received in revised form
16 December 2009
Accepted 17 December 2009
Available online 4 January 2010

Keywords:
Layered cobaltite oxide
Cathode
Proton conductor
PCFC
Y-doped $BaCeO_3$

ABSTRACT

Misfit-type $Ca_{3-x}La_xCo_4O_{9+\delta}$ (x=0, 0.3) oxides were synthesised to be evaluated as possible cathode materials for proton conducting fuel cells (PCFCs) based on $BaCe_{0.9}Y_{0.1}O_{3-\delta}$ (BCY10) dense ceramic electrolyte. The electrical conductivity value of $Ca_{2.7}La_{0.3}Co_4O_{9+\delta}$ ($\sigma \approx 53\,S\,cm^{-1}$ at 600 °C) is in the range of usually required value for a cathode application (about 50–100 $S\,cm^{-1}$). In order to test the performance of each compound as cathode material, impedance measurements were carried out on $Ca_{3-x}La_xCo_4O_{9+\delta}/BaCe_{0.9}Y_{0.1}O_{3-\delta}/Ca_{3-x}La_xCo_4O_{9+\delta}$ symmetrical half cells over the temperature range 400–800 °C under wet air. A promising electrocatalytic activity has been observed with both compounds $Ca_3Co_4O_{9+\delta}$ and $Ca_{2.7}La_{0.3}Co_4O_{9+\delta}$. Factually, the area specific resistance obtained was about 2.2 $\Omega\,cm^2$ at 600 °C.

1. Introduction

Nowadays solid oxide fuel cells (SOFCs) are attracting considerable attention. They are considered as one of the alternative energy production way that could solve the energy supplying in specific conditions (remote sites, rescue systems, domestic applications, etc.). The challenge for the different research teams is to lower the operating temperature of SOFCs from 900–1000 °C down to 600–700 °C. The fabrication cost is then expected to be reduced which would facilitate the commercialisation of such energy-conversion devices. Among the SOFCs, proton conducting fuel cells (PCFCs) are promising technology due to their working temperature range (500–700 °C). However, only few reports deal with PCFC technology and especially cathode materials for PCFCs in the literature [1–3]. In this context, our main goal is then to find out and test new cathode materials for PCFCs.

In the last two decades, cobaltite oxides have been widely studied due to the fact that many of these compounds show good electric conductivity and remarkable thermoelectric properties that could be used in practical applications. Among these oxides, the misfit layered cobaltite $Ca_3Co_4O_{9+\delta}$ ($\delta \approx 0.37$ for ideal structure) is considered as a strong candidate [4]. $Ca_3Co_4O_{9+\delta}$ was first synthesised in 1968 [5]. Its structure consists in alternating layers of a distorted CaO–CoO–CaO rock–salt-type layer and a CdI_2-type CoO_2 layer stacked along the c-axis direction [6]. Partial substitutions of Ca for alkali metals (Li, Na, K), alkaline earth metals (Sr, Ba), rare earth metals (La, Nd, Gd, Dy, etc.), Bi or Tl have been performed in order to improve its thermoelectric performances [7–13]. To our knowledge, nothing was reported on evaluating $Ca_3Co_4O_{9+\delta}$ as possible cathode material in intermediate temperature fuel cell systems. Thus, we have investigated the synthesis and the electrochemical characterisation of $Ca_3Co_4O_{9+\delta}$ and the 10% lanthanum doped $Ca_3Co_4O_{9+\delta}$. Indeed, it has been shown that the substitution of La for Ca increases significantly the electronic conductivity of $Ca_3Co_4O_{9+\delta}$ [11] In the present work, $Ca_3Co_4O_{9+\delta}$ and $Ca_{2.7}La_{0.3}Co_4O_{9+\delta}$ were applied on symmetrical half cells using $BaCe_{0.9}Y_{0.1}O_{3-\delta}$ (BCY10) as electrolyte then electrochemical characterisations were performed by impedance spectroscopy.

2. Experimental

2.1. Synthesis

Two different synthesis routes were used to prepare pure calcium cobaltite oxide and lanthanum substituted compounds. The cobaltite oxide $Ca_3Co_4O_{9+\delta}$ was prepared by solid state reaction route starting from stoichiometric mixture of $CaCO_3$ and Co_3O_4 powders (Co_3O_4 was obtained by heating $CoCO_3$ at 450 °C for 12 h under oxygen gas flow). The powder was ground, pelletised and fired at 800 °C for 10 h and at 900 °C for 50 h with intermediate grindings.

* Corresponding author.
E-mail address: mauvy@icmcb-bordeaux.cnrs.fr (F. Mauvy).

0022-4596/$ - see front matter © 2010 Elsevier Inc. All rights reserved.
doi:10.1016/j.jssc.2009.12.014

The 10% lanthanum doped cobaltite oxide was prepared by nitrate self-combustion synthesis. The interest of this route is the very low amount of impurity than the one obtained by classical solid state synthesis. Furthermore, a shorter heating treatment and less grindings are necessary to incorporate lanthanum into the $Ca_3Co_4O_{9+\delta}$ structure. A mixture of $CaCO_3$, La_2O_3 and $Co(NO_3)_2 \cdot 6H_2O$ were dissolved thoroughly in nitric acid with the nominal composition of $Ca_{2.7}La_{0.3}Co_4O_{9+\delta}$. The solution was stirred, heated at 70 °C for 15 h and dried at 300 °C. The dried mixture was calcinated at 800 °C for 40 h and at 900 °C for 24 h with intermediate grindings. During this last step, a pellet was made to ensure a total reaction. The progress of all the reactions was followed by powder X-ray diffraction.

Commercially available powder from Marion Technology Company was used for the electrolyte material $BaCe_{0.9}Y_{0.1}O_{3-\delta}$ (BCY10). This powder was uniaxially pressed into pellet form (20 mm in diameter and 1–2 mm thick), then isostatically pressed (2 kbar) and finally sintered at 1450 °C for 12 h, in air, in order to achieve a high relative density (compactness $\geq$ 94%).

2.2. Structure and X-ray diffraction studies

The $Ca_3Co_4O_{9+\delta}$ compound is a misfit-layered oxide consisting in two monoclinic subsystems with identical a, c, and β parameters, but different b parameters: a=4.8376(7) Å, c=10.833(1) Å, β=98.06(1)°, b_1=4.5565(6) Å, and b_2=2.8189(4) Å. The structure is built up from the stacking along c of triple rock salt-type layers Ca_2CoO_3 (first subsystem) with single CdI_2-type CoO_2 layers (second subsystem) (Fig. 1). As the ratio b_1/b_2=1.613 is close to 13/8, one could consider a commensurate superstructure as a first approximation to describe the structure with a=4.8376 Å, $b \approx 8b_1 \approx 13b_2$=36.479 Å, c=10.833 Å and β=98.06°. Such supercell implies an ideal composition $Ca_3Co_{3.94}O_{9.37}$ [6].

The final $Ca_3Co_4O_{9+\delta}$ and $Ca_{2.7}La_{0.3}Co_4O_{9+\delta}$ samples were characterised using X-ray powder diffraction technique. The data were collected at room temperature over the 2θ angle range 5–80° with a step size of 0.02° using a Philips X-pert diffractometer operating with Cu$K\alpha_1$ radiation. A full pattern profile matching refinement was performed using the JANA2000 program package [14]. The background was calculated with a Legendre function, and the peak shapes were described by a pseudo-Voigt function. The refinement of peak asymmetry was performed using four Berar–Baldinozzi parameters [15]. This allowed to check the purity of the $Ca_3Co_4O_{9+\delta}$ sample and to detect the presence of a small amount ($<$3%) of the $La_{1-x}Ca_xCoO_{3-\delta}$ perovskite-type phase in the $Ca_{2.7}La_{0.3}Co_4O_{9+\delta}$ sample. The full pattern profile matching performed by considering a commensurate structure (S.G. $P2_1/m$) led to the following cell parameters: a=4.832 Å, $b \approx 8b_1 \approx 13b_2$=36.467 Å, c=10.819 Å, β=98.05° and V=1887.43 Å^3 for $Ca_3Co_4O_{9+\delta}$ and a=4.841 Å, $b \approx 8b_1 \approx 13b_2$=36.467 Å, c=10.833 Å, β=97.87° and V=1894.25 Å^3 for La-doped $Ca_3Co_4O_{9+\delta}$ Fig. 2a). The increase of the cell volume is in good agreement with the replacement of Ca^{2+} by a slightly bigger La^{3+} atom. These parameters are similar to those reported for $Ca_3Co_4O_{9+\delta}$ [6]: a=4.8376 Å, $b \approx 8b_1 \approx 13b_2$=36.479 Å, c=10.833 Å, β=98.06° and V=1892.82 Å^3. In the commensurate structure, the b cell parameter is very large ($b \approx$ 36.479 Å), which

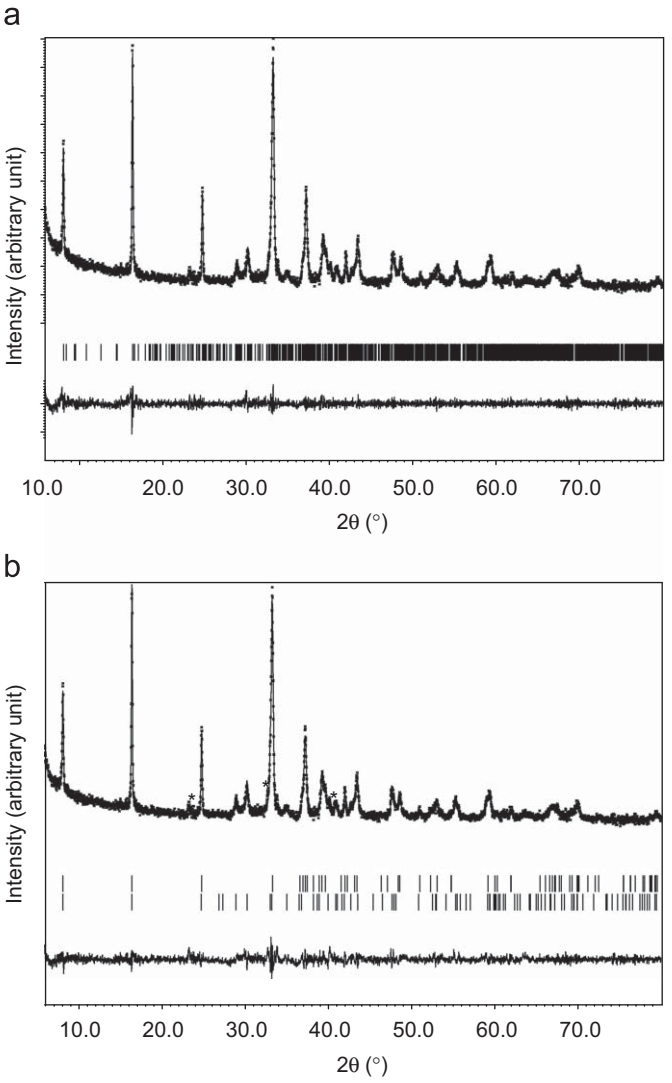

Fig. 2. (a) Final observed, calculated and difference plots for the X-ray powder diffraction (XRPD) profile refinement of $Ca_{2.7}La_{0.3}Co4O_{9+\delta}$. A commensurate structure model is considered. (b) Final observed, calculated and difference plots for the X-ray powder diffraction (XRPD) profile refinement of $Ca_{2.7}La_{0.3}Co_4O_{9+\delta}$ (peaks marked with an asterisk indicate impurities: perovskite). A misfit structure model with CoO_2 (upper) and Ca_2CoO_3 (lower) subsystems is considered.

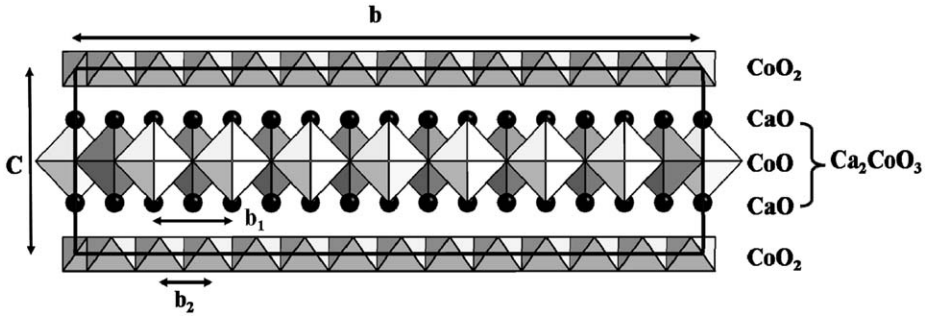

Fig. 1. Proposed structural model for final observed $Ca_3Co_4O_{9+\delta}$ involving a supercell with b–$8b_1$–$13b_2$.

induces the presence of a huge number of Bragg peaks especially at high θ angles. This makes the identification of the impurities impossible. For that reason a full pattern profile matching using two subsystems was performed (Fig. 2b).

2.3. Cathode–electrolyte chemical reactivity

The chemical reactivity between the cathode and electrolyte was at first studied in order to evidence the possible formation of a phase during the high temperature firing. The solid state reaction between the cobaltite oxides and the electrolyte $BaCe_{0.9}Y_{0.1}O_{3-\delta}$ (BCY10) were investigated by mixed powders.

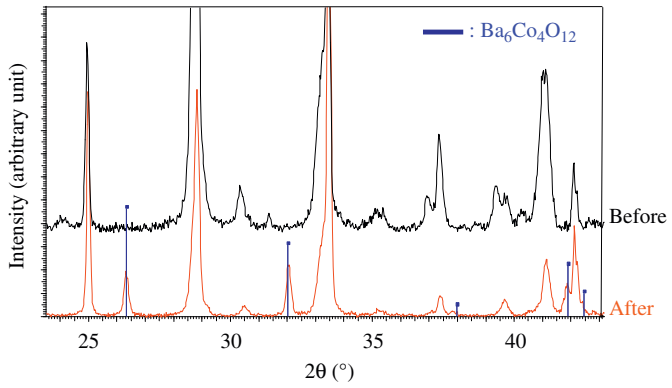

Fig. 3. X-ray powder diffraction patterns before and after the heating cycle(2 h at 850 °C) of $Ca_{2.7}La_{0.3}Co_4O_{9+\delta}$+$BaCe_{0.9}Y_{0.1}O_{3-\delta}$ (BCY10) mixture.

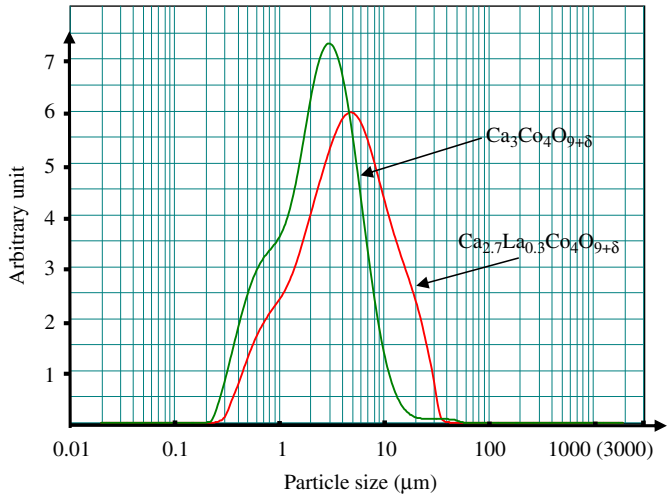

Fig. 4. Particle size distributions of $Ca_3Co_4O_{9+\delta}$ and $Ca_{2.7}La_{0.3}Co_4O_{9+\delta}$ powders.

Fine powders of cathode and electrolyte materials were thoroughly mixed in a 1:1 molar ratio, then pressed as pellets and fired at 700 °C for 2 h and at 850 °C for 2 h. These experiments have shown no reactivity at 700 °C whereas at 850 °C there is a clear evidence of the formation of a non-negligible amount of the new phase $Ba_6Co_4O_{12}$ for both cases, (BCY10) with doped and undoped cobaltite oxides. The X-ray diffraction patterns before and after the heating cycles are shown in Fig. 3.

2.4. Microscopy of the symmetrical half cells and laser particle size analysis

Fig. 4 shows the particle size distribution of $Ca_3Co_4O_{9+\delta}$ and $Ca_{2.7}La_{0.3}Co_4O_{9+\delta}$ obtained using laser particle size analysis (LPSA) after synthesis. The median size of $Ca_3Co_4O_{9+\delta}$ and $Ca_{2.7}La_{0.3}Co_4O_{9+\delta}$ particules is 2.4 and 4.2 μm, respectively. This is in contradiction with the SEM micrograph observations (the grains sizes of $Ca_3Co_4O_{9+\delta}$ are slightly bigger than those of $Ca_{2.7}La_{0.3}Co_4O_{9+\delta}$. This contradiction could be due to the presence of aggregates in $Ca_{2.7}La_{0.3}Co_4O_{9+\delta}$ sample.

Figs. 5 and 6 report scanning electron microscope (SEM) images of symmetrical half cells: cell#1, $Ca_{2.7}La_{0.3}Co_4O_{9+\delta}$/BCY10/$Ca_{2.7}La_{0.3}Co_4O_{9+\delta}$ and cell#2, $Ca_3Co_4O_{9+\delta}$/BCY10/$Ca_3Co_4O_{9+\delta}$, respectively after the sintering step of the electrode on the electrolyte pellet. The cells were sharply broken in the investigated section in order to study the different microstructures of the cathode, the electrolyte and the intermediate region. In Figs. 5a and 6a, detailed views of the cross sections of the tested cells are reported. The different cathodes (Figs. 5b and 6b) are characterised by their porous structures with lamellar shaped grains with a relatively homogenous size. Nevertheless, it seems that the $Ca_3Co_4O_{9+\delta}$ grains are slightly bigger than those of $Ca_{2.7}La_{0.3}Co_4O_{9+\delta}$. The thickness of these cathode materials was ~43 and ~70 μm for $Ca_{2.7}La_{0.3}Co_4O_{9+\delta}$ (cell#1) and $Ca_3Co_4O_{9+\delta}$ (cell#2), respectively. Obviously, the electrolyte has a dense microstructure which confirms the high calculated density (compactness ≥94%) for BCY10. It can be noticed that a very thin layer exists in between the cathode and the electrolyte for both cells (Figs. 5c and 6c). However, our EDX analyses were not efficient enough to perform accurate quantitative analysis to determine the chemical composition of these intermediate.

3. Results and discussion

3.1. DC four probes measurements

The total electrical conductivity of polycrystalline $Ca_3Co_4O_{9+\delta}$ dense pellets (compactness ≥94%) was measured in the temperature range 50–750 °C, at increasing and decreasing temperature (2 °C min^{-1}), under dry and wet air (air: H_2O–97:3),

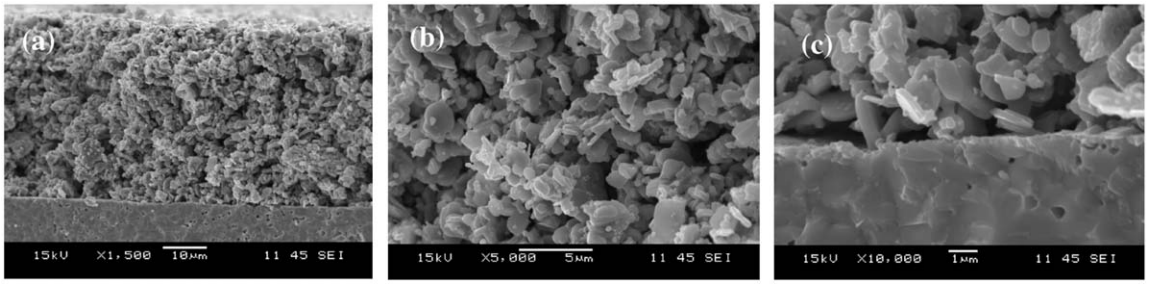

Fig. 5. (a) Scanning electron microscope (SEM) images of the symmetrical cell cross-section ($Ca_{2.7}La_{0.3}Co_4O_{9+\delta}$/BCY10/$Ca_{2.7}La_{0.3}Co_4O_{9+\delta}$), (b) detail of the cathode microstructure, and (c) zoom of the region close to the electrolyte.

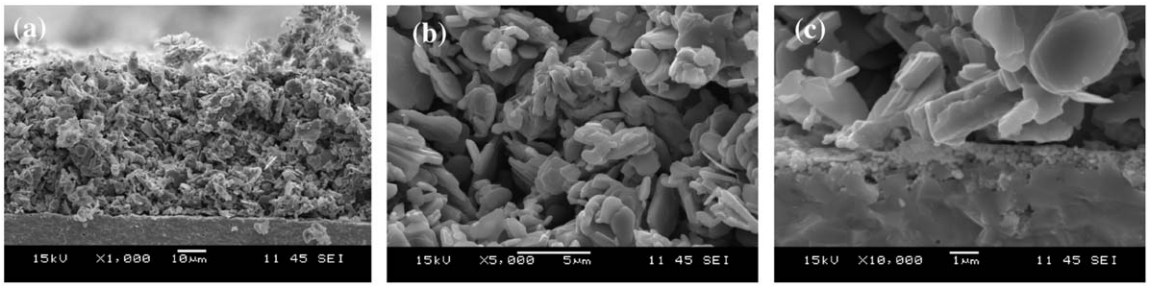

Fig. 6. (a) Scanning electron microscope (SEM) images of the symmetrical cell cross-section ($Ca_3Co_4O_{9+\delta}$/BCY10/$Ca_3Co_4O_{9+\delta}$), (b) detail of the cathode microstructure, zoom of the region close to the electrolyte.

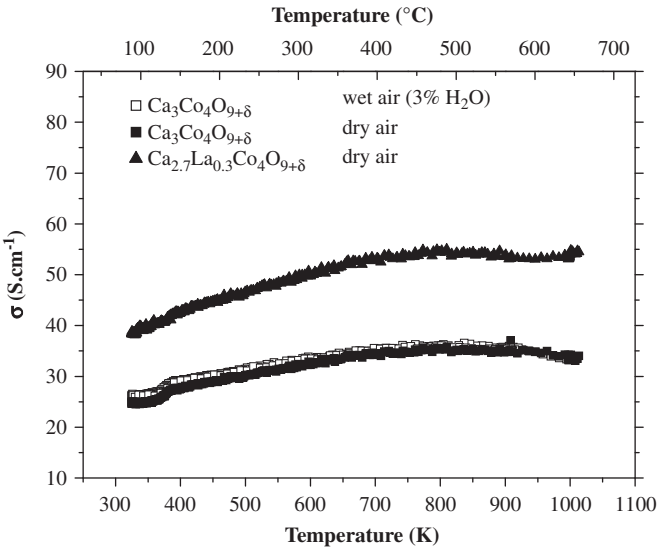

Fig. 7. Thermal variation of the electrical conductivity σ for $Ca_3Co_4O_{9+\delta}$ (square) and $Ca_{2.7}La_{0.3}Co_4O_{9+\delta}$ (triangle) compounds ($300 \le T(K) \le 1000$) under dry (solid symbol) and wet air (open symbol).

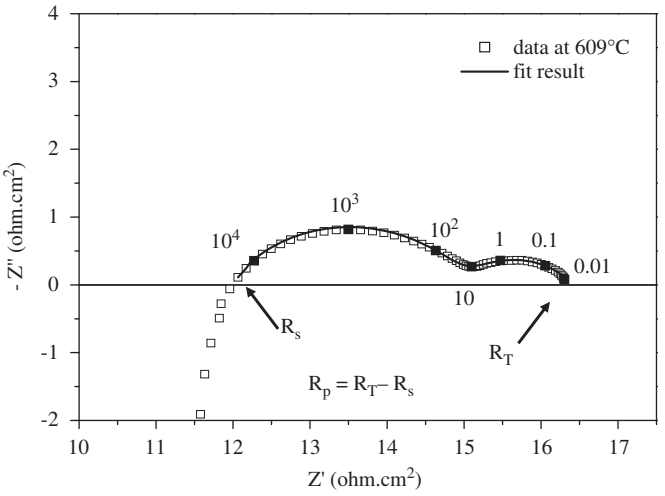

Fig. 8. A typical complex impedance spectrum recorded at 609 °C under wet air flow for a symmetrical cell ($Ca_3Co_4O_{9+\delta}$/BCY10/$Ca_3Co_4O_{9+\delta}$).The numbers above the solid squares indicate the frequencies in Hertz.

using the four-probe dc technique [16]. The thermal variation of the total electrical conductivity of $Ca_3Co_4O_{9+\delta}$ is reported in Fig. 7. The electrical conductivity is almost constant over the whole temperature range 100–750 K. This is very similar to the results reported by Masset et al. [6]. The electrical conductivity value $\sigma \approx 33\,S\,cm^{-1}$ at 600 °C is in the range of usually required value for a cathode application (about 50–100 $S\,cm^{-1}$). Data obtained on $Ca_{2.7}La_{0.3}Co_4O_{9+\delta}$ give higher electrical conductivity ($\sigma = 53\,S\,cm^{-1}$ at 600 °C) than the non-doped compound. According to these results, it can be concluded that the lanthanum doping modified significantly the total conductivity mainly governed by electronic carriers. One can also see that modifying the working atmosphere (from dry to wet air) does not have any influence on the electrical conductivity. This phenomenon can be attributed to the chemical stability of the compounds and a low influence of the ionic concentration to the total conductivity.

3.2. Electrochemical impedance spectroscopy

The $Ca_3Co_4O_{9+\delta}$ and $Ca_{2.7}La_{0.3}Co_4O_{9+\delta}$ powders were mixed with polyethylene glycol to make inks which were deposited on the circular faces of the sintered BCY10 pellets by means of a brush. The electrodes were then fired at 850 °C for 2 h. This thermal treatment is adapted to provide good adhesion to the electrolyte material and to avoid the decomposition of the cobaltite oxides. Indeed, it is well known that $Ca_3Co_4O_{9+\delta}$ decomposes at 925 °C [17]. The impedance measurements were carried out using an autolab frequency response analyser PGSTAT 302 over the temperature range 400–800 °C in humidified flowing air (air:H_2O–97:3).Before each measurement, the samples were equilibrated at constant temperature for 2–5 h. The impedance measurements were made during two subsequent heating and cooling runs. The signal amplitude was 50 and a 0 mV dc bias was used. A typical example of Nyquist diagram measured on symmetrical cell under wet air at 609 °C is reported in Fig. 8. A curve fitting was systematically performed using the Zview software. Most of the impedance diagrams recorded in this study can be decomposed, in the frequency range 1 MHz–0.01 Hz, into two loops: MF and LF for middle and low frequency range, respectively. The associated electrical equivalent circuit consist of two parallel combination of a resistance and a constant phase element (CPE: $Z_{CPE} = 1/Y^0(j\omega)^n)$) associated with a serial resistance R_S: $R_S + (R_{HF}//CPE_{HF}) + (R_{LF}//CPE_{LF})$. With respect to the associated semi circles, the equivalent capacitance C_{eq} have been calculated by the help of the relation: $C_{eq} = R^{(1-n)/n} \times CPE^{1/n}$. Equivalent capacitance values of $C_{eq}^{HF} = 6.2\ 10^{-5}$ F and $C_{eq}^{LF} = 0.2$ F resulting from the fitting at 609 °C and according to literature data [20], one can assign these contributions to the electrochemical reaction at the electrode and to the gas diffusion through the electrode, respectively. The fact that the equivalent capacities are independent of temperature leads to confirmation of the presence of two different electrochemical phenomena.

In the high temperature range, electrode polarisation resistance is mainly observed in the LF region whereas an inductive effect due to the connecting wires is measured in the HF

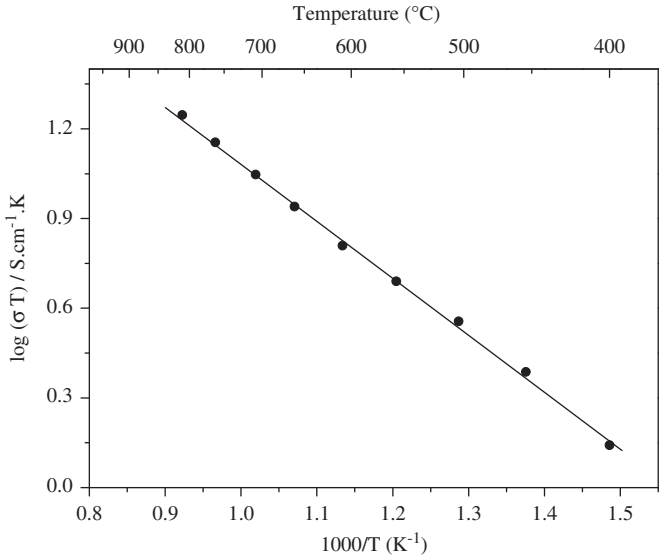

Fig. 9. Arrhenius plot of the electrical conductivity of $BaCe_{0.9}Y_{0.1}O_{3-\delta}$, in wet air, with $Ca_3Co_4O_{9+\delta}$ as cathode material.

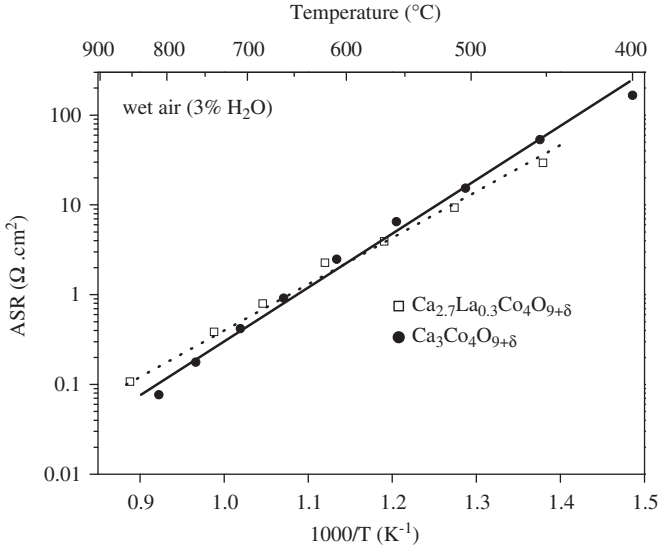

Fig. 10. Arrhenius plots of the ASR for $Ca_3Co_4O_{9+\delta}$ and $Ca_{2.7}La_{0.3}Co_4O_{9+\delta}$.

region (Fig. 8). It can be assumed that the serial resistance R_S is primary due to the electrolyte resistance insofar as the electrode ohmic resistance and the contact resistance are negligibly small. Thus, the electrolyte resistance has been deduced from the high-frequency intercept along the real axis of the Nyquist plots to calculate the BCY10 conductivity. The relation used for the calculations was $\sigma = l/(R_B \times S)$ where l, S and R_B correspond to the electrolyte thickness, the electrolyte surface area and the bulk resistance, respectively. Fig. 9 shows the plot of $\log(\sigma T)$ as a function of $1/T$ for the half cell ($Ca_3Co_4O_{9+\delta}$/BCY10/$Ca_3Co_4O_{9+\delta}$). The sample exhibit apparent Arrhenius-type T-dependencies of BCY10 conductivities, with activation energies of 36.5 kJ mol^{-1}. The conductivity of 0.007 S cm^{-1} at 600 °C for BCY10 is in agreement with values reported by Iwahara et al. (0.009 [18] and 0.016 S cm^{-1} [19]).

Fig. 10 shows the thermal variation of the area specific resistivities (ASR) which were calculated by the relation ASR = Rp × S/2, Rp being the electrodes polarisation resistance (Rp = R_{HF} + R_{LF}) equal to $R_T - R_S$ (Fig. 8) and S the surface area of both symmetrical electrodes. The value of 2.2 Ω cm^2 of the ASR obtained at 600 °C for both cathodes is very interesting. By comparison between $Ca_3Co_4O_{9+\delta}$ and $Ca_{2.7}La_{0.3}Co_4O_{9+\delta}$ ASR, it can be noticed on Fig. 10 that the difference in the total conductivity (see Fig. 7) has no significant influence on the electrocatalytic activity of the electrode. Furthermore this value can be improved by optimising some parameters as the grain size, the microstructure or the deposition process (serigraphy, spin coating, deep coating, etc.). Indeed, it is well known that the cathode material performances are very dependent on these parameters [21].

4. Conclusion

In the present work, the $Ca_3Co_4O_{9+\delta}$ and $Ca_{2.7}La_{0.3}Co_4O_{9+\delta}$ powders were prepared by solid state and nitrate auto-combustion routes, respectively. The electrical conductivity value measured on dense pellets is in the range of usually required value for a cathode application for both compounds: $\sigma > 30$ S cm^{-1} at 600 °C. These cathode materials were deposited on Y-doped $BaCeO_3$ by painting technique and then fired at 850 °C for 2 h. The scattering electron microscope analyses have shown a good adhesion of the cathode materials to $BaCe_{0.9}Y_{0.1}O_{3-\delta}$ (BCY10). The electrochemical characterisations were performed by electrochemical impedance spectroscopy and demonstrated the good potential of the cobaltite layered oxides as cathode material (ASR = 2.2 Ω cm^2 at 600 °C). Even if the total conductivity levels are different for $Ca_3Co_4O_{9+\delta}$ and $Ca_{2.7}La_{0.3}Co_4O_{9+\delta}$, the polarisation resistance measured in the range are nearly the same. Lastly, it is expected that optimising the cathodes shaping (grain size, microstructure and deposition process) will improve their electrochemical performances.

References

[1] H. Yamaura, T. Ikuta, H. Yahiro, G. Okada, Solid State Ionics 176 (2005) 269–274.
[2] Y. Lin, R. Ran, Y. Zheng, Z. Shao, W. Jin, N. Xu, J. Ahn, J. Power Sources 180 (2008) 15–22.
[3] H. Iwahara, T. Yajima, T. Hibino, H. Ushida, J. Electrochem. Soc. 140 (1993) 1687–1691.
[4] S. Li, R. Funahashi, I. Matsubara, K. Ueno, S. Sodeoka, H. Yamada, Chem. Mater. 12 (2000) 2424–2427.
[5] C. Brisi, P. Rolando, Ann. Chim (Rome) 58 (1968) 676.
[6] A.C. Masset, C. Michel, A. Maignan, M. Hervieu, O. Toulemonde, F. Studer, B. Raveau, J. Hejtmanek, Phys. Rev. B 62 (2000) 166–175.
[7] G. Xu, R. Funahashi, M. Shikano, I. Matsubara, Y. Zhou, Appl. Phys. Lett. 80 (2002) 3760–3762.
[8] I. Matsubara, R. Funahashi, T. Takeuchi, S. Sodeoka, J. Appl. Phys. 90 (2001) 462–465.
[9] D. Wang, L. Chen, Q. Wang, J. Li, J. Alloys. Compd. 376 (2004) 58–61.
[10] H. Minami, K. Itaka, H. Kawaji, Q.J. Wang, H. Koinuma, M. Lippmaa, Appl. Surf. Sci. 197-198 (2002) 442–447.
[11] J. Nan, J. Wu, Y. Deng, C.-W. Nan, Solid State Commun. 124 (2002) 243–246.
[12] S. Li, R. Funahashi, I. Matsubara, H. Yamada, K. Ueno, S. Sodeoka, Ceram. Int. 27 (2001) 321–324.
[13] J. Pei, G. Chen, D.Q. Lu, P.S. Liu, N. Zhou, Solid State Commun. 146 (2008) 283–286.
[14] V. Petricek, M. Dusek, The Crystallographic Computing System Jana, Institute of Physics, Praha, Czech Republic, 2000.
[15] J.F. Berar, G. Baldinozzi, J. Appl. Crystallogr. 26 (1993) 128.
[16] P. Dordor, E. Marquestaut, C. Salducci, P. Hagenmuller, Phys. Appl. 20 (1985) 795.
[17] E. Woermann, A. Muan, J. Inorg. Nucl. Chem. 32 (1970) 1455–1459.
[18] G. Ma, T. Shimura, H. Iwahara, Solid State Ionics 110 (1998) 103–110.
[19] K. Katahira, Y. Kohchi, T. Shimura, H. Iwahara, Solid State Ionics 138 (2000) 91–98.
[20] F. Mauvy, C. Lalanne, J.-M. Bassat, J.-C. Grenier, H. Zhao, L. Hua, P. Stevens, J. Electrochem. Soc. 153 (2006) A1547–A1553.
[21] K.C. Wincewicz, J.S. Cooper, J. Power Sources 140 (2005) 280–296.